

Dithienosilole extended BODIPYs: Synthesis and spectroscopic properties

Yijuan Sun, Lizhi Gai*, Yitong Wang, Zhirong Qu* and Hua Lu*

Key Laboratory of Organosilicon Chemistry and Material Technology, Ministry of Education, Hangzhou Normal University, Hangzhou 311121, P. R. China

Received 8 December 2018

Accepted 3 March 2019

ABSTRACT: 3,3,5-Dithienosilole-vinyl-BODIPYs were readily synthesized through Knoevenagel condensation reactions. Spectroscopic properties of two dyes in various solvents were investigated. Dyes **1** and **2** show an absorption maxima at 620 and 738 nm with absorption coefficient of 60900 and 77900 $M^{-1} \cdot cm^{-1}$ in DCM, respectively. Significant red shifts of the main spectral bands are observed relative to that of the parent 1,3,5,7-tetramethyl-BODIPY. TD-DFT calculations reproduce the spectral shifts and experimental spectra.

KEYWORDS: BODIPY, dyes, spectroscopic properties, DFT calculations.

INTRODUCTION

Fluorophores with absorption and emission wavelengths in the near-infrared (NIR) region (650–900 nm, biological window) are especially attractive for *in vivo* imaging due to deep tissue penetration of NIR light and small background autofluorescence of biomacromolecules in the living systems [1–3]. Among popular chromophores, Boron-dipyrromethene (4,4-difluoro-4-bora-3a,4a-diaza-sindacene, BDP or BODIPY) fluorescent dyes, a family of well-known luminescent compounds, have drawn much attention with their fascinating structural and attractive photophysical properties such as high fluorescence quantum yield, large absorption coefficient, considerably high photostability and chemical stability and good solubility in common solvents of different polarity [4–9]. However, the spectral properties of the common BODIPY dyes are typically limited to the 470–530 nm region [4–7].

Until now, shifts of the main spectral band into the red or NIR region have been developed through aryl, ethynylaryl and styryl substitution at the 1-, 3-, 5-, and/or 7-positions, aromatic ring fusion, by replacing the *meso*-carbon atom with an nitrogen atom to form an

aza-BODIPY [4–7, 10–11]. In particular, modification with functional building blocks at the 3,5-positions can endow them with excellent NIR photophysical and optoelectronic properties. For examples, our group developed a novel “turn-on” fluorescent probe based on a BODIPY fluorophore to detect hypoxia, by attaching a styryl substituent with a hydroxyl and nitro group at 3-position of the BODIPY core [12]. Mack and Nyokong prepared electrospun polystyrene (PS) nanofibers embedded with thienylvinyl-BODIPY for the photocatalytic degradation of azo dyes [13]. Dithienosilole (DTS), a silicon-bridged electron-rich planar tricyclic π system, is a promising electron-donating building block for efficient donor material, which possess a $\sigma^*-\pi^*$ conjugation between the silicon σ bonds and the bithiophene π system, resulting in a unique low-lying lowest unoccupied molecular orbital (LUMO) level [14–16]. It has been widely used as efficient donor units of conjugated D–A oligomers and polymers for organic electronic device materials such as OPVs, OFETs, dye-sensitized solar cells, and organic light-emitting diodes [15–18].

In this paper, 3,3,5-dithienosilole-vinyl-BODIPYs are readily synthesized *via* Knoevenagel condensation reactions between 1,3,5,7-tetramethyl BODIPY and dithienosilole-based aromatic aldehyde. The push–pull interaction is expected to narrow the HOMO–LUMO gap, resulting in a large red shift of the main spectral

*Correspondence to: Lizhi Gai, email: lizhigai@hznu.edu.cn; email: Zhirong Qu, quzr@hznu.edu.cn and Hua Lu, email: hualu@hznu.edu.cn.

band. TD-DFT calculations are performed in order to explore the effect of DTS moiety and structure–property correlations.

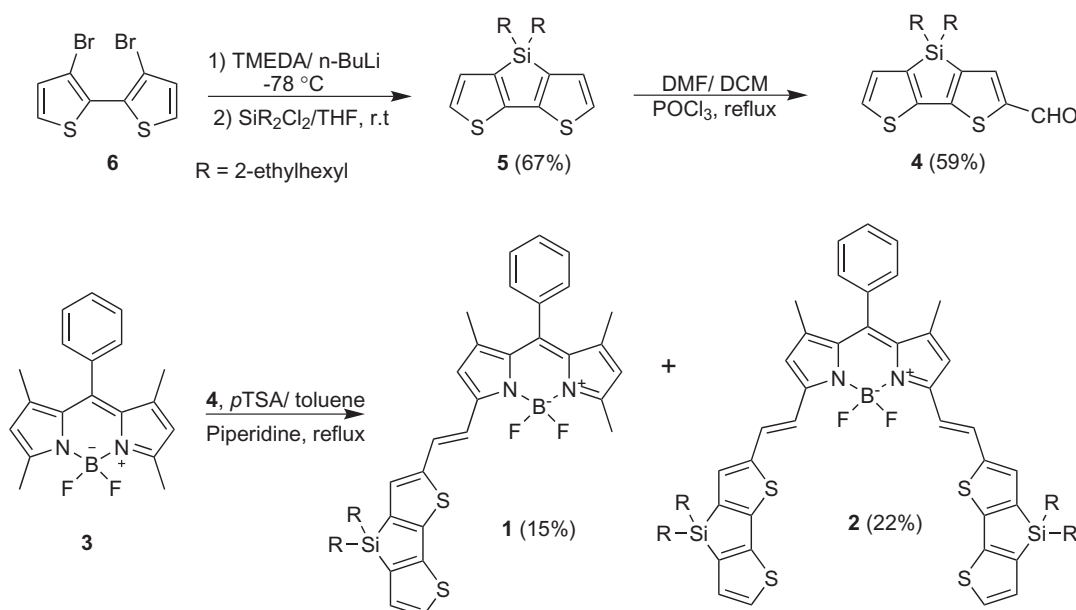
RESULTS AND DISCUSSION

The synthetic route of **1** and **2** is depicted in Scheme 1. The synthesis of 3,3'-dibromo bithiophene (**6**) and the classic BODIPY **3** were reported in the literature [19]. With **6** as a starting material, after double Br/Li-exchange, the reaction mixture was reacted with dichlorobis(2-ethylhexyl)silane to generate **5** in 67% isolated yield [20]. Compound **4** was synthesized *via* Vilsmeier–Haack reaction between **5** and DMF/POCl₃ in moderate yield [21]. Finally, the target dyes **1** and **2** were readily prepared *via* Knoevenagel condensation reaction of the classic BODIPY **3** and **4** under an atmosphere of *p*-TSA and piperidine in toluene. The structures of target products **1** and **2** were characterized by ¹H NMR, ¹³C NMR, ¹⁹F NMR, ¹¹B NMR and high resolution mass spectrometry (HR-MS) (see supporting information). All compounds are fairly stable under air and moisture both in solution and in the solid state.

Absorption and emission spectra in different solvents are presented in Figs 1 and 2, and detailed photophysical data are collected in Table 1. Dyes **1** and **2** show an absorption maxima at 620 and 738 nm with maximum absorption coefficient of 60900 and 77900 M⁻¹·cm⁻¹ in DCM, respectively. In general, the maxima absorption band can be attributed as typical of a S₀→S₁ transition with a shoulder at the high-energy side and owing to the 0–1 vibrational band of the same transition. In contrast to the absorption spectra of the precursor BODIPY (λ_{abs} = 501 nm), dramatic bathochromic shift of 119 nm for **1**;

237 nm for **2** were observed, indicative of the effect of the greater extent of the π conjugation by incorporation of DTS moieties. It should be noted that **2** shows intense absorption peaks at 457 nm, which can be attributed to the strong S₀–S₃ and S₀–S₄ transition and is associated with the π–π* excited state of DTS moieties. The absorption maxima do not show any particular trend as a function of solvent polarity. The emission bands of **1** and **2** exhibit mirror symmetry with the absorption band. The emission bands are dependent on solvent polarity and show a hypsochromic shift of approximately 31 nm (**1**) and 18 nm (**2**) with increasing solvent polarity from hexane to MeCN. **1** exhibits moderate fluorescence, whereas only very weak emission is observed for **2** in all investigated solvents, due to double internal conversion probability induced by more vibrational coupling, which enhances the rate of intersystem crossing of the dyes [22, 23]. The fluorescence decay profiles of dyes could be described by a single-exponential fit (fluorescence lifetime in the range of 1.29–7.10 ns) in all of the solvents investigated, similar to the lifetime data of other BODIPY systems published in the literature [24].

The introduction of vinyl groups at the 3-positions or 3,5-positions of BODIPY chromophore produces a greater bathochromic shift, extending the π conjugation through the 3-positions or 3,5-positions in the reported literature [7, 10, 25–27]. Compared with the absorption of classic BODIPY **3**, the 3,5-vinyl groups of modification BODIPY **2a–2c**, had larger red shifts with increasing molar extinction coefficients (Scheme 2), which can be attributed to a narrowing of the HOMO–LUMO gap due to enhanced delocalization of the π electrons in vinyl groups and functional π conjugation rings [7, 10, 25–27]. In addition, dye **2** had low quantum yield related to that



Scheme 1. Synthesis and chemical structures of BODIPY 1–2

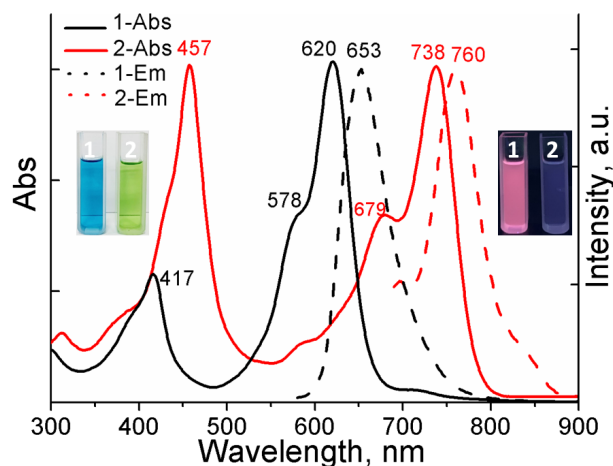


Fig. 1. The absorption and emission spectra of **1** and **2** in DCM. Photographs of **1** and **2** in DCM under visible (left) and excited at 365 nm using a UV lamp (right)

of **2a–2c**, due to the presence of a thiophene group in the DTS moiety at the 3,5-positions, which increases the rate of nonradiative decay.

In order to gain deeper insight into the electronic structures and observed photophysical properties, DFT

and TD-DFT calculations were performed using the B3LYP functional and 6-31G (*d, p*) basis sets of the Gaussian09 software package [28]. The analysis of the TD-DFT wave function had S_0-S_1 transitions mainly composed of HOMO to LUMO transitions. The HOMO are almost effectively spread over the entire molecule (Fig. 3), however, the LUMO mostly localizes on the BODIPY π system and less on the DTS fragment, indicating that weak ICT transition occurs from the donor DTS unit to the BODIPY π system. The DTS extension stabilizes LUMO and destabilizes HOMO, thus effectively narrowing the energy gap, leading to a bathochromic shift compared with the spectral band position of the parent BODIPY **3**. The lowest-energy excitations of **1** and **2** are predicted to lie at 584 and 725 nm with oscillator strengths of 1.18 and 0.78, respectively, consistent with the maxima absorption band (Table 2). The wavelengths of the third/fourth lowest energy transitions closely match the experimental data around 400 nm. Therefore, TD-DFT calculations explain the absorption spectra well (Fig. 4).

In summary, the synthesis, characterization, and theoretical analysis of dithienosilole-vinyl-BODIPY dyes have been described. The introduction of dithienosilole-vinyl groups is clearly promising for designing NIR

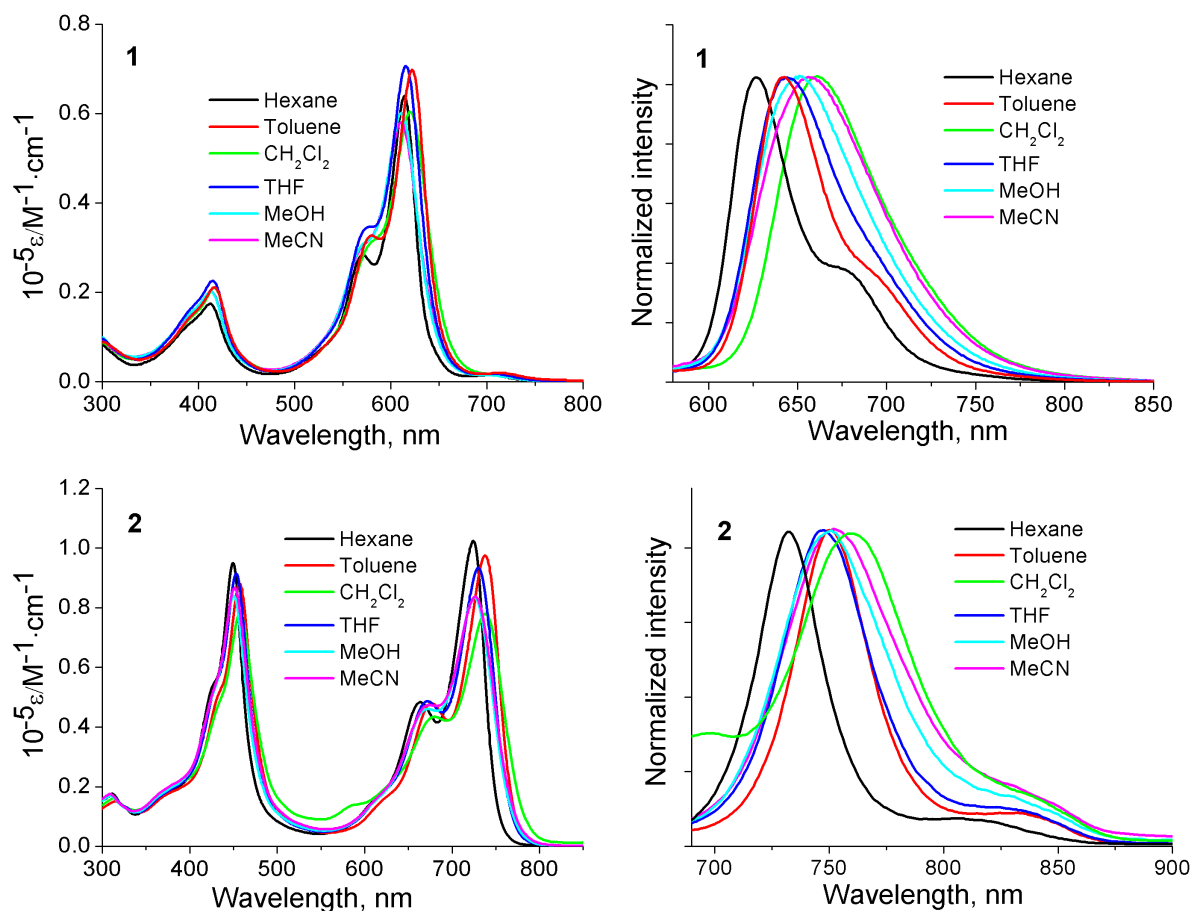
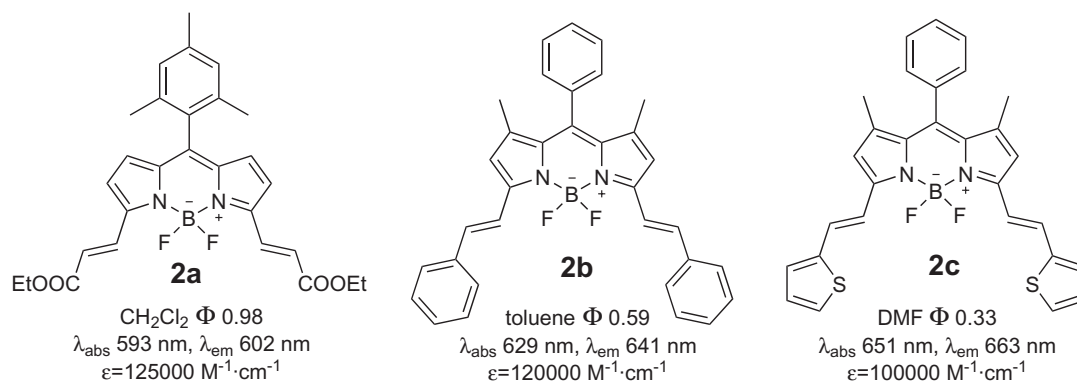
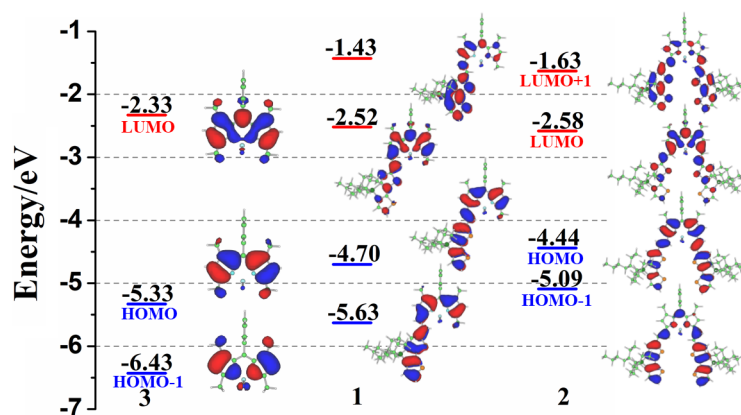


Fig. 2. The absorption (left) and emission (right) spectra of **1** and **2** in different solvents

Table 1. Spectroscopic and photophysical properties of dyes **1–2** in DCM at 298K

Dyes	Solvent	λ_{abs} [nm]	ϵ [$\text{M}^{-1} \cdot \text{cm}^{-1}$]	λ_{ems} [nm]	$\Delta\nu_{\text{abs-em}}$ [cm^{-1}]	τ [ns]	Φ_{F}	K_{r} [10^8 s^{-1}]	K_{nr} [10^8 s^{-1}]
1	Hexane	619	64100	622	78	1.97	0.46	2.34	2.74
	Toluene	621	70100	636	380	1.82	0.47	2.58	2.91
	DCM	620	60900	653	815	1.29	0.34	2.64	5.12
	THF	615	71500	639	611	2.27	0.41	1.81	2.59
	MeOH	609	59900	643	868	2.01	0.24	1.19	3.78
	MeCN	610	58000	653	1080	2.46	0.27	1.09	2.97
2	Hexane	724	102400	731	132	6.81	0.03	0.04	1.43
	Toluene	738	97500	751	235	7.10	0.02	0.03	1.38
	DCM	738	77900	760	392	6.81	0.01	0.02	1.45
	THF	730	93400	746	294	5.51	0.02	0.04	1.78
	MeOH	725	83300	750	460	3.27	0.01	0.03	3.03
	MeCN	727	83700	749	404	4.95	0.01	0.02	2.01

**Scheme 2.** The structure and photophysical data of the reported 3,5-divinyleneBODIPY dyes **2a–2c****Fig. 3.** The energy level diagram for the frontier π -MOs of the **1–3** using the B3LYP functional with 6-31G(*d*, *p*) basis sets. The angular nodal patterns are shown at an isosurface value of 0.02 a.u.

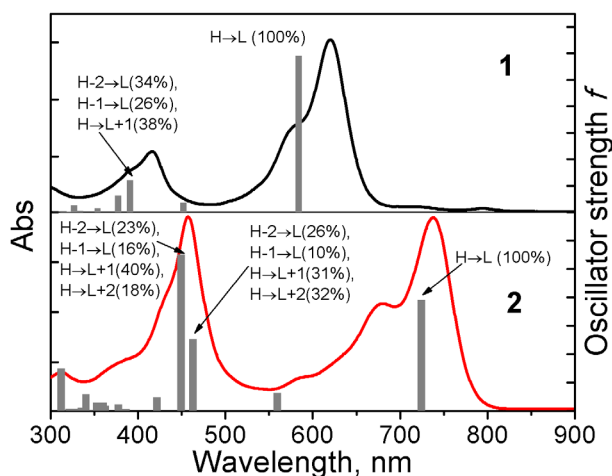
materials. Density functional calculations on energy-minimized structures reproduce experimentally observed data and trends. In this system, σ bonds of silicon in a DTS moiety is not involved in HOMO and LUMO

orbitals, therefore, silicon plays a minor role relating to the spectral shift. Research on direct orbital interaction between σ^* of silicon and π^* of BODIPY core is under way.

Table 2. Calculated electronic excitation energies, oscillator strengths, and eigenvectors for the TD-DFT spectra of the dye **1–3** carried out using the B3LYP functional with 6-31G(*d, p*) basis sets

	State ^a	Energy (eV)	λ (nm)	f^b	Orbitals (coefficient) ^c
3	S1	3.03	409	0.47	H→L (95%)
	S2	3.44	361	0.09	H-1→L (93%), H→L (7%)
1	S1	2.12	584	1.18	H→L (100%)
	S2	2.74	452	0.07	H-1→L (55%), H→L+1 (43%)
	S3	3.17	391	0.24	H-2→L (34%), H-1→L (26%), H→L+1 (38%)
2	S1	1.71	725	0.78	H→L (100%)
	S2	2.22	560	0.13	H-1→L (72%), H→L+1 (27%)
	S3	2.68	463	0.50	H-2→L (26%), H-1→L (10%), H→L+1 (31%), H→L+2 (32%)
	S4	2.76	450	1.10	H-2→L (23%), H-1→L (16%), H→L+1 (40%), H→L+2 (18%)

^aExcited state. ^bOscillator strength (<0.01 are not included). ^cMOs involved in the transitions with H and L denoting the HOMO and LUMO, respectively.

**Fig. 4.** Observed and calculated TD-DFT spectra of **1–2** based on geometry optimizations using the B3LYP functional with 6-31G(*d, p*) basis sets

EXPERIMENTAL SECTION

Materials and instrumentation

All reagents were obtained from commercial suppliers and used without further purification unless otherwise indicated. All air and moisture-sensitive reactions were carried out under nitrogen atmosphere. Glassware was dried in an oven at 100 °C and cooled under a stream of inert gas before use. Dichloromethane and triethylamine were distilled over calcium hydride. ¹H NMR, ¹³C NMR, ¹⁹F NMR, ¹¹B NMR spectra were recorded on a Bruker DRX400 and Bruker DRX500 spectrometer and referenced to the residual proton signals of the

solvent. HR-MS were recorded on a Bruker Daltonics microTOF-Q II spectrometer. All the solvents employed for the spectroscopic measurements were of UV spectroscopic grade (Aldrich).

Synthesis and characterization

Synthesis of 3,3'-dibromo-2,2'-bithiophene (6). In a 150 mL round bottom flask, 3-bromothiophene (1.45 mL, 15.4 mmol) was taken with anhydrous THF (30 mL). The solution was cooled to -78 °C and lithium diisopropylamide (LDA (7.5 mL, 2 M solution) was added dropwise over 30 min. After the addition, the solution was stirred at same temperature for 1 h and CuCl₂ (4.2 g, 31 mmol) was added. The mixture was then allowed to stir at -78 °C for 1 h and then at room temperature for 4 h. The reaction was quenched with water (20 mL). The mixture was extracted with dichloromethane, washed with distilled water (20 mL), dried over anhydrous Na₂SO₄, and evaporated *in vacuo* to obtain a brown solid. The crude compound was passed through a silica gel column using (Hex/EA = 98/2) as eluent to yield **6** as a white solid. Yield: 1.4 g (59%), ¹H NMR (400 MHz; CDCl₃; Me₄Si) δ_{H} , ppm 7.42–7.41 (d, *J* = 5.2 Hz, 2 H), 7.09–7.08 (d, *J* = 5.2 Hz, 2 H).

Synthesis of 3,3'-bis(2-ethylhexyl)silylene-2,2'-bithiophene (5). At -78 °C, a solution of *n*-BuLi in hexane (1.6 M, 4.9 mL, 7.8 mmol) was added a solution of **6** (1.25 g, 3.9 mmol) in THF (20 mL). The mixture was stirred at this temperature for 1 h, then a solution of dichlorobis(2-ethylhexyl)silane (1.88 g, 5.8 mmol) in THF (10 mL) was added. This mixture was slowly allowed to warm to room temperature overnight. The reaction mixture was then poured into 60 mL water, extracted with EA (3 × 40 mL), dried over MgSO₄,

and evaporated. The residue was purified by silica gel chromatography (hexane), to give product **5** (0.925 g, 67%). ¹H NMR (400 MHz; CDCl₃; Me₄Si) δ_H, ppm 7.17 (d, *J* = 4.0 Hz, 2 H), 7.03 (d, *J* = 4.0 Hz, 2 H), 1.40–1.38 (m, 2 H), 1.25–1.14 (m, 16 H), 0.94 (t, *J* = 6.0 Hz, 4 H), 0.81 (t, *J* = 8.0 Hz, 6 H), 0.76 (t, *J* = 8.0 Hz, 6 H).

Synthesis of 4,4-bis(2-ethylhexyl)-4H-silolo[3,2-b:4,5-b']dithiophene-2-carbaldehyde (4). **5** (2.0 g, 4.79 mmol) was dissolved in DCM (20 mL) in a 100 mL round bottom flask, and then dimethylformamide (349 mg, 4.79 mmol) was added at room temperature. The resulting reaction solution was cooled to 0 °C and then POCl₃ (0.875 mL, 9.55 mmol) was added. The reaction mixture was refluxed overnight. The reaction mixture was allowed to cool down and worked up with saturated sodium acetate solution and extracted using chloroform. The organic layer was washed with water and dried over Na₂SO₄ and purified by column chromatography on silica (DCM: hexane 2/1) to get 1.3 g (59%) of **4** as a yellow oil. ¹H NMR (400 MHz; CDCl₃; Me₄Si) δ_H, ppm 9.86 (s, 1 H), 7.69 (s, 1 H), 7.38 (d, *J* = 4.0 Hz, 1 H), 7.10 (d, *J* = 4.0 Hz, 1 H), 1.38–1.37 (m, 2 H), 1.26–1.13 (m, 16 H), 0.99–0.96 (m, 4 H), 0.81–0.73 (m, 12 H).

Synthesis of DTS-BODIPY 1 and 2. A solution of **3** (162 mg, 0.5 mmol), **4** (335 mg, 0.75 mmol) and a few crystals of *p*-TsOH in a mixture of toluene (30 mL) and piperidine (1.2 mL) was placed in a round bottom flask equipped with a Dean Stark trap. The mixture was heated until it evaporated to dryness. After cooling to room temperature, the resulting mixture was dissolved in DCM and washed with water three times. The organic phase was dried over Na₂SO₄ and the solvent was evaporated under reduced pressure. The resulting crude residue was purified by silica gel flash column chromatography (15% ethyl acetate/hexane) and recrystallized from DCM/Hexane to provide **1** as a purple solids (59 mg, 15%) and **2** as dark blue solids in 22% yield.

1: ¹H NMR (400 MHz; CDCl₃; Me₄Si) δ_H, ppm 7.49–7.48 (m, 3 H), 7.39 (s, 1 H), 7.36 (s, 1 H), 7.32–7.30 (m, 2 H), 7.25 (s, 1 H), 7.05 (d, *J* = 4.0 Hz, 1 H), 7.05 (d, *J* = 4.0 Hz, 1 H), 6.56 (s, 1 H), 5.99 (s, 1 H), 2.60 (s, 3 H), 1.43 (s, 2 H), 1.42 (s, 3 H), 1.39 (s, 3 H), 1.26–1.15 (m, 16 H), 0.96 (t, *J* = 6.0 Hz, 4 H), 0.83 (t, *J* = 8.0 Hz, 6 H), 0.77 (t, *J* = 8.0 Hz, 6 H). ¹³C NMR (100 MHz; CD₂Cl₂; Me₄Si) δ_C, ppm 152.77, 143.19, 143.03, 135.46, 133.55, 132.55, 131.84, 130.63, 129.78, 129.52, 128.80, 128.64, 127.00, 125.84, 125.15, 124.37, 121.53, 119.39, 117.95, 117.23, 36.34, 36.04, 34.54, 31.58, 30.56, 30.11, 29.26, 23.35, 23.12, 18.02, 14.53, 14.29, 10.95. ¹¹B NMR (128 MHz; CDCl₃; Me₄Si) δ_B, ppm 0.97 (t, *BF*₂) ppm. ¹⁹F NMR (376 MHz; CDCl₃; Me₄Si) δ_F, ppm -142.43 (q, *BF*₂). UV-vis (DCM): λ_{max}, nm (log ε) 620 (4.78); MS (HRMS-ESI): *m/z* 775.3541 (calcd. for [M + H]⁺ 775.3537).

2: ¹H NMR (400 MHz; CDCl₃; Me₄Si) δ_H, ppm 7.55–7.51 (m, 3 H), 7.43–7.41 (m, 3 H), 7.38–7.36 (m, 3 H), 7.33–7.30 (m, 2 H), 7.24 (s, 2 H), 7.13 (d, *J* = 4.0 Hz,

2 H), 6.64 (s, 2 H), 1.46 (s, 6 H), 1.44–1.40 (m, 4 H), 1.25–1.18 (m, 32 H), 1.02 (t, *J* = 6.0 Hz, 8 H), 0.84 (t, *J* = 8.0 Hz, 12 H), 0.78 (t, *J* = 8.0 Hz, 12 H). ¹³C NMR (100 MHz; CD₂Cl₂; Me₄Si) δ_C, ppm 152.29, 149.40, 145.01, 144.96, 144.82, 144.09, 142.36, 135.65, 132.47, 130.59, 129.49, 129.33, 129.17, 127.12, 118.19, 117.38, 36.39, 36.11, 36.08, 32.44, 30.15, 29.34, 29.32, 23.41, 23.12, 18.08, 14.82, 14.36. ¹¹B NMR (128 MHz; CDCl₃; Me₄Si) δ_B, ppm 1.19 (t, *BF*₂) ppm. ¹⁹F NMR (376 MHz; CDCl₃; Me₄Si) δ_F, ppm -138.74 (q, *BF*₂). UV-vis (DCM): λ_{max}, nm (log ε) 738 (4.89); MS (HRMS-ESI): *m/z* 1162.5709 (calcd. for [M-F]⁺ 1162.5765).

Spectroscopic measurements

UV-vis absorption spectra were recorded on a Shimadzu 1800 spectrophotometer. The fluorescence lifetimes and the absolute quantum yields (Φ_F) of the samples were determined with a Horiba Jobin Yvon Fluorolog-3 spectrofluorimeter. Absorption and emission measurements were carried out in 1 × 1 cm quartz cuvettes. For all measurements, the temperature was kept constant at (298 ± 2) K. Dilute solutions with absorbance of less than 0.05 at the excitation wavelength were used for the measurement of fluorescence quantum yields. 9,10-Diphenylanthracene was used as the standard ZnPc (Φ = 0.28, in DMF) [29]. The quantum yield, Φ, was calculated using equation (1): [30]

$$\Phi_{\text{sample}} = \Phi_{\text{std}} \left[\frac{I_{\text{sample}}}{I_{\text{std}}} \right] \left[\frac{A_{\text{std}}}{A_{\text{sample}}} \right] \left[\frac{n_{\text{sample}}}{n_{\text{std}}} \right]^2 \quad (1)$$

where the *sample* and *std* subscripts denote the sample and standard, respectively, *I* is the integrated emission intensity, *A* stands for the absorbance, and *n* is refractive index.

DFT calculations

The G09W software package was used to carry out DFT geometry optimization using the B3LYP functional with 6-31G (*d, p*) basis sets [28]. The same approach was used to calculate the absorption properties based on the time-dependent (TD-DFT) method.

Acknowledgments

Financial support was provided by the National Natural Science Foundation of China (Nos. 21801057, 21871072, 21501073). Research funding project of Hangzhou Normal University (2018PYXML009, 2018QDL002, 2018YLXK16). Theoretical calculations were carried out at the Computational Center for Molecular Design of Organosilicon Compounds, Hangzhou Normal University.

Supporting information

¹H NMR, ¹³C NMR, ¹⁹F NMR, ¹¹B NMR and HR-MS spectra are given in the supplementary material. This

material is available free of charge via the Internet at <http://www.worldscinet.com/jpp/jpp.shtml>.

REFERENCE

- Guo Z, Park S, Yoon J and Shin I. *Chem. Soc. Rev.* 2014; **43**: 16–29.
- Yuan L, Lin W, Zheng K, He L and Huang W. *Chem. Soc. Rev.* 2013; **42**: 622–661.
- Weissleder R and Ntziachristos V. *Nat. Med.* 2003; **9**: 123–128.
- Wang J, Li J, Chen N, Wu Y, Hao EH, Wei Y, Mu X and Jiao LJ. *New J. Chem.* 2016; **40**: 5966–5975.
- Loudet A and Burgess K. *Chem. Rev.* 2007; **107**: 4891–4932.
- Boens N, Leen V and Dehaen W. *Chem. Soc. Rev.* 2012; **41**: 1130–1172.
- Lu H, Mack J, Yang Y and Shen Z. *Chem. Soc. Rev.* 2014; **43**: 4778–4823.
- Kamkaew A, Lim SH, Lee HB, Kiew LV, Chung LY and Burgess K. *Chem. Soc. Rev.* 2013; **42**: 77–88.
- Osati S, Ali H and Lier JE. van. *J. Porphyrins Phthalocyanines* 2016; **20**: 61–75.
- Harris J, Gai LZ, Kubheka G, Mack J, Nyokong T and Shen Z. *Chem. — Eur. J.* 2017; **23**: 14507–14514.
- Lu H, Shimizu S, Mack J, You XZ, Shen Z and Kobayashi N. *Chem. — Asian J.* 2011; **6**: 1026–1037.
- Wang SS, Liu H, Mack J, Tian JW, Zou B, Lu H, Li ZF, Jiang JX and Shen Z. *Chem. Commun.* 2015; **51**: 13389–13392.
- Lebechia A K, Gai LZ, Shen Z, Nyokong T and Mack J. *J. Porphyrins Phthalocyanines* 2018; **22**: 1–8.
- Zeng W, Cao Y, Bai Y, Wang Y, Shi Y, Zhang M, Wang F, Pan C and Wang C. *Chem. Mater.* 2010; **22**: 1915–1925.
- Ohshita J. *Macromol. Chem. Phys.* 2009; **210**: 1360–1370.
- Tanaka D, Ohshita J, Ooyama Y and Morihara Y. *Polym. J.* 2013; **45**: 1153–1158.
- Hou J, Chen HY, Zhang S, Li G and Yang Y. *J. Am. Chem. Soc.* 2008; **130**: 16144–16145.
- Ni W, Li M, Liu F, Wan XJ, Feng HR, Kan B, Zhang Q, Zhang HT and Chen YS. *Chem. Mater.* 2015; **27**: 6077–6084.
- Aghazada S, Gao P, Yella A, Marotta G, Moehl T, Teuscher J, Moser J-E, Angelis F De, Grätzel M and Nazeeruddin MK. *Inorg. Chem.* 2016; **55**: 6653–6659.
- Oosterhout SD, Savikhin V, Zhang JX, Zhang YD, Burgers MA, Marder SR, Bazan GC and Toney MF. *Chem. Mater.* 2017; **29**: 3062–3069.
- Xiang WC, Gupta A, Kashif MK, Duffy N, Bilic A, Evans RA, Spiccia L and Bach U. *ChemSusChem* 2013; **6**: 256–260.
- Gai, LZ, Lu H, Zou B, Lai GQ, Shen Z and Li ZF. *RSC Adv.* 2012; **2**: 8840–8846.
- Bañuelos-Prieto J, Agarrabeitia AR, García-Moreno I, López-Arbeloa I, Costela A, Infantes L, Perez-Ojeda ME, Palacios-Cuesta M and Ortiz MJ. *Chem. — Eur. J.* 2010; **16**: 14094–14105.
- Ventura B, Marconi G, Bröring M, Krüger R and Flamigni L. *New J. Chem.* 2009; **33**: 428–438.
- Chen J, Mizumura M, Shinokubo H and Osuka A. *Chem. — Eur. J.* 2009; **15**: 5942–5949.
- Rurack K, Kollmannsberger M and Daub J. *New J. Chem.* 2001; **25**: 289–292.
- Huang L, Yu X, Wu W and Zhao J. *Org. Lett.* 2012; **14**: 2594–2597.
- Gaussian 09, Revision C.01, Frisch MJ, Trucks GW, Schlegel HB, Scuseria GE, Robb MA, Cheeseman JR, Scalmani G, Barone V, Mennucci B, Petersson GA, Nakatsuji H, Caricato M, Li X, Hratchian HP, Izmaylov AF, Bloino J, Zheng G, Sonnenberg JL, Hada M, Ehara M, Toyota K, Fukuda R, Hasegawa J, Ishida M, Nakajima T, Honda Y, Kitao O, Nakai H, Vreven T, Montgomery JA, Jr, Peralta JE, Ogliaro F, Bearpark M, Heyd JJ, Brothers E, Kudin KN, Staroverov VN, Kobayashi R, Normand J, Raghavachari K, Rendell A, Burant JC, Iyengar SS, Tomasi J, Cossi M, Rega N, Millam JM, Klene M, Knox JE, Cross JB, Bakken V, Adamo C, Jaramillo J, Gomperts R, Stratmann RE, Yazyev O, Austin AJ, Cammi R, Pomelli C, Ochterski JW, Martin RL, Morokuma K, Zakrzewski VG, Voth GA, Salvador P, Dannenberg JJ, Dapprich S, Daniels AD, Farkas Ö, Foresman JB, Ortiz JV, Cioslowski J and Fox DJ. Gaussian, Inc., Wallingford CT, 2009.
- Scalise I and Durantini EN. *Bioorg. Med. Chem.* 2005; **13**: 3037–3045.
- Lakowicz J. *Principles of Fluorescence Spectroscopy*, SpringerVerlag, New York, 3rd edn, 2006.